



On some upwind difference schemes for the phenomenological sedimentation-consolidation model

R. BÜRGER and K. HVISTENDAHL KARLSEN¹

*Institute of Mathematics A, University of Stuttgart, Pfaffenwaldring 57, 70569 Stuttgart, Germany
(e-mail: buerger@mathematik.uni-stuttgart.de)*

¹*Department of Mathematics, University of Bergen, Johs. Brunsgt. 12, N-5008 Bergen, Norway (e-mail: kennethk@mi.uib.no)*

Received 26 June 2000; accepted in revised form 5 January 2001

Abstract. In one space dimension, the phenomenological sedimentation-consolidation model reduces to an initial-boundary value problem (IBVP) for a nonlinear strongly degenerate convection-diffusion equation with a non-convex, time-dependent flux function. The frequent assumption that the effective stress of the sediment layer is a function of the local solids concentration only which vanishes below a critical concentration value causes the model to be of mixed hyperbolic-parabolic nature. Consequently, its solutions are discontinuous and entropy solutions must be sought. In this paper, first a (short) guided visit to the mathematical (entropy solution) framework in which the well-posedness of this and a related IBVP can be established is given. This also includes a short discussion of recent existence and uniqueness results for entropy solutions of IBVPs. The entropy solution framework constitutes the point of departure from which numerical methods can be designed and analysed. The main purpose of this paper is to present and demonstrate several finite-difference schemes which can be used to correctly simulate the sedimentation-consolidation model in civil and chemical engineering and in mineral processing applications, *i.e.*, conservative schemes satisfying a discrete entropy principle. Here, finite-difference schemes of upwind type are considered. To some extent, also stability and convergence properties of the proposed schemes are discussed. Performance of the proposed schemes is demonstrated by simulation of two cases of batch settling and one of continuous thickening of flocculated suspensions. The numerical examples focus on a detailed error study, an illustration of the effect of varying the initial datum, and on simulation of practically important thickener operations, respectively.

Key words: sedimentation, flocculated suspension, degenerate parabolic equation, entropy solution, finite-difference scheme

1. Introduction

In this contribution, we consider the quasilinear strongly degenerate parabolic equation

$$\frac{\partial u}{\partial t} + \frac{\partial g(u, t)}{\partial x} = \frac{\partial^2 A(u)}{\partial x^2}, \quad (1)$$

where

$$A(u) := \int_0^u a(s) \, ds, \quad a(u) \geq 0, \quad g(u, t) := q(t)u + f(u),$$

on a cylinder $Q_T := \Omega \times \mathcal{T}$, $\Omega := (0, 1)$, $\mathcal{T} := (0, T)$, $T > 0$. We allow that $a(u)$ vanishes on an interval $[0, u_c]$ of solution values, where Equation (1) is of hyperbolic type, and that $a(u)$ is discontinuous at $u = u_c$.

Equation (1) and these assumptions are motivated by the model of sedimentation-consolidation processes of flocculated suspensions presented in [1, 2]. In this model, $f(u) = f_{bk}(u)$ denotes the Kynch batch-flux density function, $q(t)u$ is a convective flux related to the discharge control, and the diffusion coefficient $a(\cdot)$ accounts for compressibility effects.

We consider two different initial-boundary-value problems. Problem A consists of Equation (1) together with a given initial distribution of solution values, a Dirichlet boundary condition at one boundary, and a particular nonlinear flux condition at the second. This problem has been studied previously by Bürger and Wendland [3] and recently by Bürger *et al.* [4]. The second IBVP, Problem B, is obtained from Problem A if the Dirichlet boundary condition is replaced by a second flux boundary condition. These boundary conditions are stated precisely in Section 2.1.

Problem B as a variant of Problem A has been included in the more recent analysis [4]. In the context of the sedimentation-consolidation model, it is assumed in Problem A that a concentration value can be directly prescribed at $x = 1$ and that at $x = 0$ the total volumetric solids flux $g(u, t) + \partial A(u)/\partial x$ is reduced to its convective part $q(t)u$. The alternative formulation, Problem B, stipulates that at $x = 1$ the total volumetric solids flux is prescribed as a ‘feed flux’ $\Psi(t)$. In both cases, we assume that an initial concentration distribution $u_0(x)$ is known. We come back to this model in Section 4.

It is well known that, due to both the degeneracy of the diffusion coefficient $a(u)$ and to the nonlinearity of the flux density function $f(u)$, solutions of Equation (1) are in general discontinuous and have to be considered as entropy solutions. A numerical scheme that approximates entropy solutions of Problems A or B should therefore have the built-in property to reproduce these discontinuities appropriately without the necessity to track them explicitly, *i.e.* the scheme should be shock capturing. Moreover, an obvious requirement is that the scheme should approximate (converge to) the correct (entropy) solution of the problem it is trying to solve. This clearly rules out classical schemes based on naive finite differencing for strictly parabolic equations, which otherwise work well for smooth solutions, see [5]. It is the purpose of this paper to present examples of working finite-difference schemes having all these desired properties and which are moreover easy to implement.

We emphasize that the main purpose of this paper is to present and demonstrate numerical methods that can be used by the practitioners in chemical and civil engineering and mineral processing to simulate sedimentation-consolidation processes. However, the appropriate design of numerical methods in the present context is intimately connected to the mathematical framework in which the models are well posed. Therefore we devote Section 2 to a discussion of the mathematical (entropy solution) framework for Problems A and B. In particular, we outline recent existence and uniqueness results for entropy solutions of Problems A and B which take into account the fact that we admit a discontinuous diffusion coefficient $a(\cdot)$. This requires a new approach for the uniqueness proof, since the available proof by Wu and Yin [6] presupposes that $a(\cdot)$ is Lipschitz continuous. In fact, most, but not all, constitutive equations suggested for the sedimentation-consolidation model do lead to a discontinuous diffusion coefficient $a(\cdot)$.

Equipped with the well-posedness of the entropy solution, we describe in Section 3 finite difference schemes for their numerical computation, and include some recent stability and convergence results for the initial-value problem of Equation (1). Finally, we describe numerical schemes for the IBVPs A and B of the sedimentation-consolidation model.

In Section 4, we come back to that application. We first briefly outline the basic model assumptions and show that a technical assumption on Problem B will usually be satisfied. We

then present numerical solutions of three different test cases. In Section 4.2.1, we simulate a batch sedimentation process and perform an L^1 error study of the numerical schemes. In Section 4.2.2, we keep the discretization parameters fixed but vary the initial datum. In both paragraphs, which correspond to batch settling ($q \equiv 0$ and $\Psi \equiv 0$), the model parameters are chosen in such a way that numerical results can be compared to experimental data. Finally, in Section 4.2.3, we simulate a hypothetical sequence of thickener operations by approximating an entropy solution of Problem B with $q \not\equiv 0$ and a varying feed flux $\Psi(t)$. Conclusions that can be drawn from this paper are summarized in Section 5.

2. Mathematical theory

2.1. ADDITIONAL ASSUMPTIONS AND INITIAL AND BOUNDARY CONDITIONS

In addition to the assumptions stated in Section 1, we require the flux density function $f(\cdot)$ to be at least Lipschitz continuous with $\text{supp } f \subset [0, 1]$ and $f(u) \leq 0$. The function $q(\cdot)$ is assumed to be nonpositive and Lipschitz continuous. Moreover, we require that $\text{TV}_{\mathcal{T}}(q) < \infty$ and $\text{TV}_{\mathcal{T}}(q') < \infty$.

For Problem A, the initial and boundary conditions are

$$u(x, 0) = u_0(x), \quad x \in \Omega; \quad (2)$$

$$u(1, t) = \varphi_1(t), \quad t \in \mathcal{T}; \quad (3)$$

$$\left(f(u) - \frac{\partial A(u)}{\partial x} \right) (0, t) = 0, \quad t \in \mathcal{T}. \quad (4)$$

The second IBVP, Problem B, is obtained from Problem A if the boundary condition (3) is replaced by

$$\left(g(u, t) - \frac{\partial A(u)}{\partial x} \right) (1, t) = \Psi(t), \quad t \in \mathcal{T}. \quad (5)$$

2.2. PRELIMINARIES AND NOTION OF ENTROPY SOLUTION

We seek solutions u in the space $BV(Q_T)$ of all functions $v \in L^\infty(Q_T)$ for which there exist constants $K_1, K_2 > 0$ such that the inequalities

$$\begin{aligned} \int_0^{T-\Delta t} \int_0^1 |v(x, t + \Delta t) - v(x, t)| \, dt \, dx &\leq K_1 \Delta t, \\ \int_0^T \int_0^{1-\Delta x} |v(x + \Delta x, t) - v(x, t)| \, dt \, dx &\leq K_2 \Delta x \end{aligned}$$

hold uniformly for sufficiently small $\Delta x, \Delta t > 0$.

Before introducing the notion of entropy solution for Problems A and B, respectively, we need to state some necessary assumptions on the coefficients of Equation (1) as well as the initial and boundary data. To this end, let ω_ε be a standard C^∞ mollifier with $\text{supp } \omega_\varepsilon \subset (-\varepsilon, \varepsilon)$ and define for $\varepsilon > 0$

$$a_\varepsilon(u) = ((a + \varepsilon) * \omega_\varepsilon)(u) \quad \text{and} \quad A_\varepsilon(u) := \int_0^u a_\varepsilon(s) \, ds.$$

For Problem A, the assumptions on the initial and boundary data can be stated as follows:

$$\varphi_1(t) \in [0, 1] \text{ for } t \in \overline{\mathcal{T}} \text{ and } \varphi_1 \text{ has a finite number of local extrema;} \quad (6)$$

$$u_0 \in \left\{ z \in BV(\Omega) : z(x) \in [0, 1]; \right. \\ \left. \exists M > 0 : \forall \varepsilon > 0 : \text{TV} \left(\frac{\partial A_\varepsilon(z)}{\partial x} \right) < M \right\}, \quad (7)$$

while for Problem B we require that (7) is valid and that either $\Psi \equiv 0$ or that

$$\exists \xi, M_g > 0 : \forall u \in \text{supp } f : \xi a(u) \geq q(t) + \sup_{v \in \text{supp } f} \frac{f(u) - f(v)}{u - v} + M_g. \quad (8)$$

For differentiable flux-density functions, condition (8) was first used by Wu [7] to show existence of generalized solutions of a variant of Problem B under stronger regularity assumptions on the flux density function $g(\cdot, t)$ and on the diffusion coefficient $a(\cdot)$. An immediate consequence of assumption (8) is that solution values $u \leq u_c$, for which Equation (1) is hyperbolic and which therefore propagate along characteristics, propagate downwards, *i.e.*, away from the boundary $x = 1$. The same holds for a discontinuity between two approximate limits u^+ and u^- of a generalized solution of Equation (1) with $0 \leq u^-, u^+ < u_c$ if we recall that its propagation velocity $\sigma(u^-, u^+)$ is given by the Rankine-Hugoniot condition [8]

$$\sigma(u^-, u^+) = q(t) + \frac{f(u^+) - f(u^-)}{u^+ - u^-}.$$

Consequently, condition (8) ensures that no hyperbolic characteristics or shocks hit the boundary $x = 1$, on which the total flux is prescribed according to boundary condition (5). This avoids oscillations of $u(1, \cdot)$ as a function of t that otherwise occur.

We mention that Wu [7] derived condition (8) from the stronger assumption

$$\frac{\partial}{\partial u} g(u, t) = q(t) + f'(u) < 0 \quad \text{for all } 0 \leq u \leq u_c, t \geq 0, \quad (9)$$

i.e., he actually directly prescribed what we formulated as a consequence of (8). However, as we shall show in Section 4, in the context of the sedimentation-consolidation model only condition (8) is usually satisfied, in contrast to the more restrictive condition (9).

We need the assumption (7) on u_0 to ensure the existence of a solution from $BV(Q_T)$. However, if $a(\cdot)$ is sufficiently smooth (*i.e.*, at least continuous), then it is sufficient to require that $\text{TV}_\Omega(\partial_x u_0)$ (and not $\text{TV}_\Omega(\partial_x A_\varepsilon(u_0))$) is finite.

We now turn to the definitions of entropy solutions of Problem A and B, respectively. We recall from [4] that a function $u \in L^\infty(Q_T) \cap BV(Q_T)$ is an entropy solution of Problem A if the following conditions are satisfied:

$$\frac{\partial A(u)}{\partial x} \in L^2(Q_T); \quad (10)$$

$$\text{f. a. a. } t \in \mathcal{T}, \gamma_0 \left(f(u) - \frac{\partial A(u)}{\partial x} \right) = 0; \quad (11)$$

$$\text{f. a. a. } x \in \overline{\Omega}, \lim_{t \downarrow 0} u(x, t) = u_0(x), \quad (12)$$

and if for all nonnegative test functions $\varphi \in C^\infty((0, 1] \times \overline{\mathcal{T}})$ with $\text{supp } \varphi \subset (0, 1] \times \mathcal{T}$ and for all $k \in \mathbb{R}$

$$\begin{aligned} & \iint_{Q_T} \left\{ |u - k| \frac{\partial \varphi}{\partial t} + \text{sgn}(u - k) \left[g(u, t) - g(k, t) - \frac{\partial A(u)}{\partial x} \right] \frac{\partial \varphi}{\partial x} \right\} dt dx \\ & + \int_0^T \left\{ -\text{sgn}(\varphi_1(t) - k) \left[g(\gamma_1 u, t) - g(k, t) - \gamma_1 \frac{\partial A(u)}{\partial x} \right] \varphi(1, t) \right. \\ & \left. + [\text{sgn}(\gamma_1 u - k) - \text{sgn}(\varphi_1(t) - k)] [A(\gamma_1 u) - A(k)] \frac{\partial \varphi}{\partial x}(1, t) \right\} dt \geq 0. \end{aligned} \quad (13)$$

Similarly, a function $u \in L^\infty(Q_T) \cap BV(Q_T)$ is an entropy solution of Problem B if (10) and (12) are valid, if for all nonnegative $\varphi \in C_0^\infty(Q_T)$ and for all $k \in \mathbb{R}$ the inequality

$$\iint_{Q_T} \left\{ |u - k| \frac{\partial \varphi}{\partial t} + \text{sgn}(u - k) \left[g(u, t) - g(k, t) - \frac{\partial A(u)}{\partial x} \right] \frac{\partial \varphi}{\partial x} \right\} dt dx \geq 0 \quad (14)$$

holds, and if

$$\gamma_1 \left(g(u, t) - \frac{\partial A(u)}{\partial x} \right) = \Psi(t) \quad \text{for almost all } t \in \mathcal{T}. \quad (15)$$

Here, $\gamma_0 u := (\gamma u)(0, t)$ and $\gamma_1 u := (\gamma u)(1, t)$ denote the traces of u . Entropy inequalities like (13) go back to the pioneering papers of Kruřkov [9] and Vol'pert [10] for first order equations and Vol'pert and Hudjaev [11] for second-order equations.

We now briefly discuss jump and entropy boundary conditions that can be derived from the integral inequality (13), see [6, 8] for details. We first note that if u is an entropy solution of Problem A or B, then a discontinuity at a jump point $(x, t) \in Q_T$ between two approximate limits (with respect to the normal of the jump) u^+ and u^- can exist only for $0 \leq u^-, u^+ \leq u_c$, and that for $0 \leq u^-, u^+ < u_c$, the well-known Rankine–Hugoniot condition and Oleřnik's jump entropy condition E are satisfied. If one assumes in addition more regularity of the diffusion coefficient $a(\cdot)$, for example Lipschitz continuity, then the propagation velocity of a discontinuity with $0 \leq u^+ < u^- = u_c$ is given by

$$\sigma = \frac{1}{u^+ - u_c} \left[g(u^+, t) - g(u_c, t) + \lim_{\xi \uparrow x} \frac{\partial A(u)}{\partial x} \right],$$

and such a discontinuity is admissible, *i.e.*, a shock, if the jump entropy condition

$$\forall k \in [u^+, u_c] : \frac{g(u^+, t) - g(k, t)}{u^+ - k} \leq s \leq \frac{1}{k - u_c} \left[g(k, t) - g(u_c, t) + \lim_{\xi \uparrow x} \frac{\partial A(u)}{\partial x} \right]$$

holds. Analogous conditions hold for $0 \leq u^- < u^+ = u_c$.

Finally, we mention that condition (13) is satisfied if and only the integral inequality (14) holds for all nonnegative $\varphi \in C_0^\infty(Q_T)$ and $k \in \mathbb{R}$; if $a(s) = 0$ for all s between $\phi_1(t)$ and $(\gamma_1 u)(1, t)$, and if the trace $v = (\gamma_1 u)(1, t)$ satisfies the following entropy boundary inequality:

$$\forall k \in \mathbb{R} : \left[\text{sgn}(v - k) - \text{sgn}(\phi_1(t) - k) \right] \left[g(v, t) - g(k, t) - \gamma_1 \frac{\partial A(u)}{\partial x} \right] \geq 0. \quad (16)$$

This means that we cannot assume that the trace of entropy solution of Problem A satisfies the boundary condition (3) in a pointwise sense wherever $\phi_1(t) \leq u_c$; rather, we can then only require that $(\gamma_1 u)(1, t)$ belongs to the (time-dependent) set of all values v for which (16) is satisfied. The concept of entropy boundary conditions associated with this set-valued reformulation goes back to the analysis of Bardos, Le Roux and Nédélec [12] and Dubois and Le Floch [13] for first order equations.

2.3. EXISTENCE AND UNIQUENESS RESULTS

We now briefly summarize some recent results on the existence and uniqueness of entropy solutions of Problems A and B, and state a new regularity result for the integrated diffusion coefficient for entropy solutions of Problem B. For details we refer to [4].

For both problems, existence of entropy solutions can be shown by the vanishing viscosity method. To this end, we consider the regularized parabolic IBVPs

$$\frac{\partial u^\varepsilon}{\partial t} + \frac{\partial}{\partial x} (q_\varepsilon(t)u^\varepsilon + f_\varepsilon(u^\varepsilon)) = \frac{\partial^2 A_\varepsilon(u^\varepsilon)}{\partial x^2}, \quad (x, t) \in Q_T, \quad (17)$$

$$u^\varepsilon(x, 0) = u_0^\varepsilon(x), \quad x \in \Omega, \quad (18)$$

$$u^\varepsilon(1, t) = \varphi_1^\varepsilon(t), \quad (19)$$

$$\left(f_\varepsilon(u^\varepsilon) - \frac{\partial A_\varepsilon(u^\varepsilon)}{\partial x} \right) (0, t) = 0, \quad t \in (0, T], \quad (20)$$

and

$$\frac{\partial u^\varepsilon}{\partial t} + \frac{\partial}{\partial x} (q_\varepsilon(t)u^\varepsilon + f_\varepsilon(u^\varepsilon)) = \frac{\partial^2 A_\varepsilon(u^\varepsilon)}{\partial x^2}, \quad (x, t) \in Q_T, \quad (21)$$

$$u^\varepsilon(x, 0) = u_0^\varepsilon(x), \quad x \in \Omega, \quad (22)$$

$$\left(g_\varepsilon(u^\varepsilon, t) - \frac{\partial A_\varepsilon(u^\varepsilon)}{\partial x} \right) (1, t) = \Psi_\varepsilon(t), \quad (23)$$

$$\left(f_\varepsilon(u^\varepsilon) - \frac{\partial A_\varepsilon(u^\varepsilon)}{\partial x} \right) (0, t) = 0, \quad t \in (0, T], \quad (25)$$

where the functions q , f , u_0 , φ_1 and Ψ have been replaced by particular smooth approximations for each problem that ensure compatibility conditions and existence of smooth solutions. It can then be shown that there exist constants M_1 to M_5 independent of ε such that the smooth solutions of (17)–(20) satisfy

$$\|u^\varepsilon\|_{L^\infty(Q_T)} \leq M_1, \quad \left\| \frac{\partial u^\varepsilon}{\partial x}(\cdot, t) \right\|_{L^1(\Omega)} \leq M_2 \quad \forall t \in \mathcal{T}, \quad \left\| \frac{\partial u^\varepsilon}{\partial t} \right\|_{L^1(Q_T)} \leq M_3, \quad (25)$$

while those of Problem (21)–(24) satisfy

$$\|u^\varepsilon\|_{L^\infty(Q_T)} \leq M_1, \quad \left\| \frac{\partial u^\varepsilon}{\partial t}(\cdot, t) \right\|_{L^1(\Omega)} \leq M_4 \quad \forall t \in \mathcal{T}, \quad (26)$$

and, in the case where $\Psi \equiv 0$,

$$\left\| \frac{\partial u^\varepsilon}{\partial x}(\cdot, t) \right\|_{L^1(\Omega)} \leq M_5 \quad \forall t \in \mathcal{T}, \quad (27)$$

and, in the case where (8) holds,

$$\left\| \frac{\partial u^\varepsilon}{\partial x} \right\|_{L^1(Q_T)} \leq M_5. \quad (28)$$

Estimates (25) imply that the family $\{u^\varepsilon\}_{\varepsilon>0}$ of solutions of Problem (17)–(20) is bounded in $W^{1,1}(Q_T) \subset BV(Q_T)$. Hence there exists a sequence $\varepsilon = \varepsilon_n \downarrow 0$ such that $\{u^{\varepsilon_n}\}$ converges in $L^1(Q_T)$ to a function $u \in L^\infty(Q_T) \cap BV(Q_T)$. The same compactness assertion holds for the family of solutions $\{u^\varepsilon\}_{\varepsilon>0}$ of Problem B $^\varepsilon$.

To prove that u is an entropy solution of Problem A or B, it has to be shown that the diffusion function $A(u)$ has the required regularity. In both cases, it is fairly easy to show that

$$\left\| \frac{\partial A_\varepsilon(u^\varepsilon)}{\partial x} \right\|_{L^2(Q_T)} \leq M_6,$$

for some constant $M_6 > 0$ independent of ε . Therefore, passing if necessary to a subsequence as $\varepsilon \downarrow 0$, $A_\varepsilon(u^\varepsilon) \rightarrow A(u)$ strongly in $L^2(Q_T)$ and

$$\frac{\partial A_\varepsilon(u^\varepsilon)}{\partial x} \rightarrow \frac{\partial A(u)}{\partial x} \quad \text{weakly in } L^2(Q_T).$$

It is now easy to verify that the limit function u satisfies (11) to (13) or (12), (14) and (15), respectively. For the case of Problem B, the a priori regularity statement of $A(u)$ can be considerably improved; namely, we can indeed show that $A(u)$ belongs to the Hölder space $C^{1,1/2}(\overline{Q_T})$ and that $A_\varepsilon(u^\varepsilon)$ converges uniformly to $A(u)$, see [4] for details.

Finally, consider two entropy solutions u and v either of Problem A or of Problem B with initial data u_0 and v_0 , respectively. Then the inequality

$$\|u(\cdot, t) - v(\cdot, t)\|_{L^1(\Omega)} \leq \|u_0 - v_0\|_{L^1(\Omega)} \quad (29)$$

is valid, which immediately implies that both problems have at most one entropy solution. This can be shown by the ‘doubling of the variables’ device introduced first by Kružkov [9] as a tool for proving (29) for the entropy solution of scalar conservation laws and very recently extended by Carrillo [14] to a class of degenerate parabolic equations. This recent extension is adopted in [4] to Problems A and B and leads to the inequality

$$\iint_{Q_T} \left\{ |u - v| \frac{\partial \varphi}{\partial t} + \operatorname{sgn}(u - v) \left[g(u, t) - g(v, t) - \left(\frac{\partial A(u)}{\partial x} - \frac{\partial A(v)}{\partial x} \right) \right] \frac{\partial \varphi}{\partial x} \right\} dt \, dx \geq 0,$$

valid for all nonnegative test functions $\varphi \in C_0^\infty(Q_T)$, from which stability and uniqueness can be obtained as in [4], see also [8].

Summing up, we have the following theorem:

THEOREM 1. [4] *Under the assumptions specified in Section 1, both initial-boundary-value problems A and B have exactly one entropy solution $u \in BV(Q_T)$.*

It should be pointed out that the new stability and uniqueness proof detailed in [4] is *not* based on a jump condition, in contrast to the uniqueness proof by Wu and Yin [6]. In fact, it is not clear whether a jump condition can be derived with integrated diffusion functions $A(u)$ that are only Lipschitz continuous. Moreover, it has been possible to derive jump conditions only in the 1-D case so far, while the new uniqueness proof can also be extended to multi-dimensional boundary-value problems.

3. Finite-difference schemes

In this section we present some numerical methods for degenerate parabolic problems. In several papers, we have elaborated on numerical methods for the sedimentation-consolidation model based on ‘operator splitting’ [2, 15, 16, 17]. For a general introduction to operator splitting methods and a long list of relevant papers, we refer to the lecture notes [18]. In this paper, our main focus will be on finite difference schemes. The material in this section is based on a series of theoretical papers by Evje, Karlsen, and Risebro [5, 19, 20, 21, 22].

3.1. INITIAL-VALUE PROBLEM

To focus on the main ideas, we consider here the initial value problem

$$\frac{\partial u}{\partial t} + \frac{\partial f(u)}{\partial x} = \frac{\partial^2 A(u)}{\partial x^2}, \quad u(x, 0) = u_0(x), \quad (30)$$

where $(x, t) \in Q_T = \mathbb{R} \times (0, T)$, $f = f(u)$ and $A = A(u)$ are Lipschitz continuous functions with $A(\cdot)$ nondecreasing, and $u_0 \in L^1(\mathbb{R}) \cap L^\infty(\mathbb{R})$. We will return to the full sedimentation-consolidation model towards the end of this section.

Following [23], we say that u is an entropy solution of (30) if

$$u \in L^1(Q_T) \cap L^\infty(Q_T) \cap C(0, T; L^1(\mathbb{R})), \quad (31)$$

$$A(u) \in L^2(0, T; H^1(\mathbb{R})), \quad (32)$$

$$\text{f. a. a. } x \in \mathbb{R}, \quad \lim_{t \downarrow 0} u(x, t) = u_0(x), \quad (33)$$

and for all nonnegative $\varphi \in C_0^\infty(Q_T)$ and for all $k \in \mathbb{R}$ the following inequality holds:

$$\iint_{Q_T} \left\{ |u - k| \frac{\partial \varphi}{\partial t} + \text{sgn}(u - k) \left[f(u) - f(k) - \frac{\partial A(u)}{\partial x} \right] \frac{\partial \varphi}{\partial x} \right\} dt dx \geq 0. \quad (34)$$

Note that we do not need $u \in BV(Q_T)$ for the initial-value problem (30) to be well-posed. The reason that this is needed for the sedimentation-consolidation model (*cf.* Section 2), is only to ensure the existence of the boundary traces $\gamma_0 u, \gamma_1 u$. The well-posedness of the entropy solution of (30) is proved in [22]. In that paper, also the multi-dimensional initial problem with a general flux function of the type $f = f(x, t, u)$ is treated.

As is shown in [5, 21], numerical methods based on naive finite-difference formulation of the diffusion term may be adequate for smooth solutions but can give wrong results when discontinuities are present.

It turns out that central differencing of the second-order term and upwind differencing of the convective flux is preferable, in order to achieve conservative discretization of both terms.

As is well known, upwind differencing stabilizes profiles which are liable to undergo sudden changes, *i.e.*, discontinuities and other large gradient profiles. Therefore upwind differencing is perfectly suited for the treatment of the sedimentation-consolidation model.

3.1.1. First-order scheme

Select a mesh size $\Delta x > 0$, a time step $\Delta t > 0$, and an integer N so that $N\Delta t = T$, and denote the value of the difference approximation at $(x_j, t_n) = (j\Delta x, n\Delta t)$ by u_j^n , where $j \in \mathbb{Z}$ and $n = 0, \dots, N$. In this paper, we use the so-called Engquist-Osher (or generalized upwind) scheme

$$\frac{u_j^{n+1} - u_j^n}{\Delta t} + \frac{f^{\text{EO}}(u_j^n, u_{j+1}^n) - f^{\text{EO}}(u_{j-1}^n, u_j^n)}{\Delta x} = \frac{A(u_{j+1}^n) - 2A(u_j^n) + A(u_{j-1}^n)}{(\Delta x)^2}, \quad (35)$$

where the numerical flux $f^{\text{EO}}(u_j^n, u_{j+1}^n) := f^+(u_j^n) + f^-(u_{j+1}^n)$ is given by

$$f^+(u) = f(0) + \int_0^u \max(f'(s), 0) ds, \quad f^-(u) = \int_0^u \min(f'(s), 0) ds.$$

Notice that the functions $f^+(\cdot)$ and $f^-(\cdot)$ are Lipschitz continuous and, respectively, nondecreasing and nonincreasing. Moreover, the difference scheme (35) is consistent since

$$f^{\text{EO}}(u, u) = f^+(u) + f^-(u) = f(u), \quad \forall u \in \mathbb{R}. \quad (36)$$

Observe that, for a monotone flux function f , the Engquist-Osher flux takes the simplified form $f^{\text{EO}}(u_j^n, u_{j+1}^n) \equiv f(u_j^n)$ if $f' > 0$ and $f^{\text{EO}}(u_j^n, u_{j+1}^n) \equiv f(u_{j+1}^n)$ if $f' < 0$, which is the Godunov (or upwind) numerical flux. For a discussion of the relation between the Godunov and Engquist-Osher schemes, see [25]. For stability reasons, we always assume that the following CFL condition holds:

$$\text{CFL} := L_f \frac{\Delta t}{\Delta x} + 2L_A \frac{\Delta t}{(\Delta x)^2} \leq 1, \quad (37)$$

where L_f and L_A denote the Lipschitz constants of $f(\cdot)$ and $A(\cdot)$, respectively.

We remark that difference schemes for multi-dimensional convection-diffusion equations with variable (nonsmooth) coefficients are treated in [22], see also [5] for the case of source terms.

3.1.2. A convergence result

We next discuss the stability and convergence properties of the scheme (35). To this end, let $u_\Delta : Q_T \rightarrow \mathbb{R}$, $\Delta = (\Delta x, \Delta t)$, be the interpolant of degree zero associated with the discrete data points $\{u_j^n\}$:

$$u_\Delta(x, t) = u_j^n \quad \text{for } x_{j-1/2} \leq x < x_{j+1/2} \text{ and } t_n \leq t < t_{n+1},$$

where $x_j := j\Delta x$ and $t_n := n\Delta t$ for $j \in \mathbb{Z}$ and $n = 0, \dots, N-1$. For technical reasons, we extend the definition of u_Δ by the value 0 for all $t > T$. Regarding the sequence $\{u_\Delta\}$, we have:

THEOREM 2. [22] *The sequence $\{u_\Delta\}$ of difference approximations converges in $L_{loc}^1(Q_T)$ as $\Delta \downarrow 0$ to the unique entropy solution u of (30).*

Sketch of Proof. We follow [22] closely in this proof, see also [5].

First, it is not difficult to show a uniform L^∞ bound:

$$\|u_\Delta(\cdot, t)\|_{L^\infty(\mathbb{R})} \leq C_1 \quad \forall t \in (0, T), \quad (38)$$

for some constant $C_1 > 0$ independent of Δ . Next, one can easily show that the scheme (35) is L^1 contractive; i.e., if $\{u_j^n\}$ and $\{v_j^n\}$ are two finite-difference solutions with data $\{u_j^0\}$ and $\{v_j^0\}$, respectively, then

$$\sum_{j \in \mathbb{Z}} |u_j^n - v_j^n| \leq \sum_{j \in \mathbb{Z}} |u_j^0 - v_j^0|.$$

Since $u_0 \in L^1(\mathbb{R})$, it then follows that there exists a spatial modulus of continuity function ν such that

$$\|u_\Delta(\cdot + y, t) - u_\Delta(\cdot, t)\|_{L^1(\mathbb{R})} \leq \nu(|y|), \quad \forall y \in \mathbb{R}, y \rightarrow 0, \forall t \in (0, T), \quad (39)$$

where the modulus $\nu(\cdot)$ is independent of Δ . We recall that a function $\nu : [0, \infty) \rightarrow [0, \infty)$ is called modulus of continuity if it is continuous and nondecreasing with $\nu(0) = 0$.

One can now use the difference scheme (35), the spatial estimate (39) and Kružkov's interpolation lemma (see [22]) to show that there exists a temporal modulus of continuity ω such that

$$\|u_\Delta(\cdot, t + \tau) - u_\Delta(\cdot, t)\|_{L^1(\mathbb{R})} \leq \omega(\tau), \quad \forall \tau \geq 0, \tau \rightarrow 0, \forall t \in (0, T), \quad (40)$$

where the modulus is again independent of Δ .

Using the three estimates (38)–(40) and Kolmogorov's compactness lemma, it is thus possible to select a subsequence that converges in $L^1_{loc}(Q_T)$ to a limit u satisfying (31) and (33).

The next step is to show that the limit u satisfies (32). To this end, one proves the following estimate:

$$\|A(u_\Delta(\cdot + y, \cdot + \tau)) - A(u_\Delta(\cdot, \cdot))\|_{L^2(Q_T)} \leq C_2 (|y| + \sqrt{\tau}), \quad (41)$$

for $y \in \mathbb{R}$ and $\tau \geq 0$ with $y, \tau \rightarrow 0$. Here, $C_2 > 0$ is a constant independent of Δ . An application of Kolmogorov's compactness lemma then gives

$$A(u_\Delta) \rightarrow \bar{A} \quad \text{in } L^2_{loc}(Q_T) \text{ as } \Delta \rightarrow 0 \text{ and } \bar{A} \in L^2(0, T; H^1(\mathbb{R})).$$

Equipped with strong convergence $u_\Delta \rightarrow u$, we conclude that $\bar{A} = A(u)$ and thus (32) holds. We would like to mention that the proof of (41) is based on deriving so-called *weak BV* estimates. The proof is complicated by the fact that u_0 does not belong to $BV(\mathbb{R})$. Moreover, to derive (41), we actually need to impose a slightly stronger CFL condition than (37). We will not go into further details about this, but refer instead to [22].

Finally, convergence of $\{u_\Delta\}$ to the correct physical solution of (30) follows from the consistency of the scheme (see (36)) and the cell entropy inequality

$$\begin{aligned} \frac{|u_j^{n+1} - k| - |u_j^n - k|}{\Delta t} + \Delta_- \left(f^{\text{EO}}(u_j^n \vee k, u_{j+1}^n \vee k) - f^{\text{EO}}(u_j^n \wedge k, u_{j+1}^n \wedge k) \right) \\ - \Delta_- \Delta_+ |A(u_j^n) - A(k)| \leq 0, \quad \forall k \in \mathbb{R}, \end{aligned} \quad (42)$$

with the standard notation $u \vee v := \max(u, v)$, $u \wedge v := \min(u, v)$, $\Delta_- u_j := u_j - u_{j-1}$, and $\Delta_+ u_j := u_{j+1} - u_j$. This conclusion essentially mimics the proof of the Lax-Wendroff theorem. The discrete entropy inequality (42) is in turn an easy consequence of the monotonicity

of the scheme. The reader is referred to [22] for further details on the proof of Theorem 2. \square

We point out that if, we assume that u_0 is sufficiently smooth (i.e., at least $TV_\Omega(f(u_0) - \partial_x A(u_0)) < \infty$), then we also have $u \in BV(Q_T)$ and $\{A(u_\Delta)\}$ converges uniformly on compact sets $\mathcal{K} \subset Q_T$ as $\Delta \downarrow 0$ to $A(u) \in C^{1,1/2}(\overline{Q_T})$, see [5] for details. Moreover, within the BV framework, one can also analyse difference schemes for the more general case of doubly nonlinear degenerate parabolic equations, see [19].

3.1.3. Semi-implicit and implicit schemes

In many applications it is desirable to avoid the explicit stability restriction (37) associated with (30). One way to overcome this restriction is of course to use the semi-implicit scheme

$$\frac{u_j^{n+1} - u_j^n}{\Delta t} + \frac{f^{\text{EO}}(u_j^n, u_{j+1}^n) - f^{\text{EO}}(u_{j-1}^n, u_j^n)}{\Delta x} = \frac{A(u_{j+1}^{n+1}) - 2A(u_j^{n+1}) + A(u_{j-1}^{n+1})}{(\Delta x)^2}, \quad (43)$$

with the (less restrictive) CFL condition $L_f \Delta t / \Delta x \leq 1$, or the ‘CFL free’ implicit scheme

$$\begin{aligned} \frac{u_j^{n+1} - u_j^n}{\Delta t} + \frac{f^{\text{EO}}(u_j^{n+1}, u_{j+1}^{n+1}) - f^{\text{EO}}(u_{j-1}^{n+1}, u_j^{n+1})}{\Delta x} \\ = \frac{A(u_{j+1}^{n+1}) - 2A(u_j^{n+1}) + A(u_{j-1}^{n+1})}{(\Delta x)^2}. \end{aligned} \quad (44)$$

Note that (43) and (44) involve the solution of nonlinear equations. Following [21, 22], one can prove that these nonlinear equations have a unique solution and that the schemes (43) and (44) converge to the unique entropy solution of (30). The schemes (43) and (44) will not be used in this paper.

3.1.4. Second-order scheme

The upwind scheme (and all other monotone schemes) are at most first-order accurate, which leads to poor accuracy in regions where the exact solution is smooth. To overcome these problems, we use the generalized MUSCL (Variable Extrapolation) idea of van Leer [24, 25] to formally upgrade the Engquist-Osher scheme (35) to second-order accuracy. In the context of conservation laws, Van Leer observed that one can increase the spatial accuracy by replacing piecewise constant data of the Riemann problem with piecewise linear data. To this end, we introduce a piecewise linear $u^n(x)$ defined by

$$u^n(x) = u_j^n + s_j^n(x - x_j), \quad x \in (x_{j-1/2}, x_{j+1/2}),$$

where s_j^n denotes a suitable slope constructed from the available data $\{u_j^n\}$. In regions where $s_j^n = 1$, the reconstruction is linear and the truncation error is $\mathcal{O}((\Delta x)^2)$. In regions where $s_j^n = 0$, the reconstruction used is piecewise constant and the truncation error is $\mathcal{O}(\Delta x)$. The slopes are limited to enforce the monotonicity of the reconstruction. The second order scheme is identified by the choice of a limiter function that defines the slopes. There exists a variety of possible limiters, see, e.g., [26] for a discussion of limiters. Here we have used the so-called θ - limiter

$$s_j^n = \text{MM} \left(\theta \frac{u_j^n - u_{j-1}^n}{\Delta x}, \frac{u_{j+1}^n - u_{j-1}^n}{2\Delta x}, \theta \frac{u_{j+1}^n - u_j^n}{\Delta x} \right), \quad \theta \in [0, 2],$$

where MM is the Min-Mod function

$$\text{MM}(a, b, c) = \begin{cases} \min(a, b, c), & \text{if } a, b, c > 0, \\ \max(a, b, c), & \text{if } a, b, c < 0, \\ 0, & \text{otherwise.} \end{cases}$$

The next step is to extrapolate the data to the boundaries of each cell, yielding the extrapolated values

$$u_j^L := u_j^n - \frac{\Delta x}{2} s_j^n, \quad u_j^R := u_j^n + \frac{\Delta x}{2} s_j^n. \quad (45)$$

The second-order upwind scheme now takes the form

$$\frac{u_j^{n+1} - u_j^n}{\Delta t} + \frac{f^{\text{EO}}(u_j^R, u_{j+1}^L) - f^{\text{EO}}(u_{j-1}^R, u_j^L)}{\Delta x} = \frac{A(u_{j-1}^n) - 2A(u_j^n) + A(u_{j+1}^n)}{(\Delta x)^2}. \quad (46)$$

Although the proof is more difficult than in the first-order case, it can be shown that also the second-order scheme satisfies a discrete entropy condition and that it converges to the unique entropy solution of the problem [20].

We mention that to obtain a second-order time discretization (in addition to second-order spatial discretization), one can replace the forward Euler time discretization by a linear multi-step method or by a Runge-Kutta type of discretization. We will not pursue this further here.

3.2. INITIAL-BOUNDARY-VALUE PROBLEMS

Let us now turn to the description of the difference schemes for the full sedimentation-consolidation model. These difference schemes are implemented and demonstrated in the next section.

We divide the interval $\Omega = (0, 1)$ into J subintervals of length $\Delta x = 1/J$ and the time interval $\mathcal{T} = (0, T)$ into N subintervals of length $\Delta t = T/N$. As before, let u_j^n denote the approximate solution value at $(j\Delta x, n\Delta t)$. The computation starts by setting $u_j^0 = u_0(j\Delta x)$ for $j = 0, \dots, J$. The first-order interior scheme takes the form

$$\begin{aligned} \frac{u_j^{n+1} - u_j^n}{\Delta t} + q(n\Delta t) \frac{u_{j+1}^n - u_j^n}{\Delta x} + \frac{f_{\text{bk}}^{\text{EO}}(u_j^n, u_{j+1}^n) - f_{\text{bk}}^{\text{EO}}(u_{j-1}^n, u_j^n)}{\Delta x} \\ = \frac{A(u_{j+1}^n) - 2A(u_j^n) + A(u_{j-1}^n)}{(\Delta x)^2}, \quad j = 1, \dots, J-1. \end{aligned} \quad (47)$$

We assume that the following CFL condition holds:

$$L_g \frac{\Delta t}{\Delta x} + 2L_A \frac{\Delta t}{(\Delta x)^2} \leq 1, \quad L_g := \max_{t \in [0, T]} |q(t)| + L_{f_{\text{bk}}},$$

where $L_{f_{\text{bk}}}$ denotes the Lipschitz constant of f_{bk} . Introducing extrapolated values (45) for $j = 1, \dots, J-1$, the second order (in space) interior scheme takes the form

$$\begin{aligned} \frac{u_j^{n+1} - u_j^n}{\Delta t} + q(n\Delta t) \frac{u_{j+1}^L - u_j^R}{\Delta x} + \frac{f_{\text{bk}}^{\text{EO}}(u_j^R, u_{j+1}^L) - f_{\text{bk}}^{\text{EO}}(u_{j-1}^R, u_j^L)}{\Delta x} \\ = \frac{A(u_{j+1}^n) - 2A(u_j^n) + A(u_{j-1}^n)}{(\Delta x)^2}, \quad j = 1, \dots, J-1. \end{aligned} \quad (48)$$

The boundary condition (4) prescribed at $x = 0$ is discretized by evaluating the formula (47) for the interior scheme for $j = 0$ and setting

$$\left(f_{\text{bk}}(u) - \frac{\partial A(u)}{\partial x} \right) (0, n\Delta t) \approx f_{\text{bk}}^{\text{EO}}(u_{-1}^n, u_0^n) - \frac{A(u_0^n) - A(u_{-1}^n)}{\Delta x} = 0,$$

whence we obtain the updating formula for the value u_0^n

$$\frac{u_0^{n+1} - u_0^n}{\Delta t} + q(n\Delta t) \frac{u_1^n - u_0^n}{\Delta x} + \frac{f_{\text{bk}}^{\text{EO}}(u_0^n, u_1^n)}{\Delta x} = \frac{A(u_1^n) - A(u_0^n)}{(\Delta x)^2},$$

which is used for both the first and second-order schemes. Note that this formulation avoids referring to an artificial solution value u_{-1}^n . The boundary condition at $x = 1$ for Problem A is implemented simply by setting $u_J^n = \varphi_1(n\Delta t)$, while that for Problem B (see (5)) is approximated by setting

$$q(n\Delta t)u_J^n + f_{\text{bk}}^{\text{EO}}(u_J, u_{J+1}) - \frac{A(u_{J+1}^n) - A(u_J^n)}{\Delta x} = \Psi(n\Delta t),$$

which yields

$$\frac{u_J^{n+1} - u_J^n}{\Delta t} + \frac{\Psi(n\Delta t) - q(n\Delta t)u_J^n}{\Delta x} - \frac{f_{\text{bk}}^{\text{EO}}(u_{J-1}^n, u_J^n)}{\Delta x} = \frac{A(u_{J-1}^n) - A(u_J^n)}{(\Delta x)^2}.$$

4. Application to the sedimentation-consolidation model

4.1. INTRODUCTION

The study of degenerate convection-diffusion equations is in part motivated by a model of sedimentation-consolidation processes of flocculated suspensions in an idealized sedimentation vessel, which is here considered to be of height 1 [m]. In that application, $u = u(x, t)$ denotes the local volumetric solids concentration, $q(t) \leq 0$ is the average flow velocity of the mixture which can be controlled externally (for example by prescribing the mixture volumetric discharge rate at $x = 0$), $f_{\text{bk}}(u)$ is a given nonlinear function relating the local solid-fluid relative velocity to the local solids concentration, and

$$a(u) = -\frac{f_{\text{bk}}(u)\sigma'_e(u)}{\Delta \varrho g u}, \quad (49)$$

where $\Delta \varrho > 0$ denotes the solid-fluid mass density difference, g is the acceleration of gravity, and $\sigma'_e(u) \geq 0$ is the derivative of the solid effective stress function. The material behaviour of the suspension is thus described by the functions $f_{\text{bk}}(u)$ and $\sigma_e(u)$. This sedimentation-consolidation model is described in detail in [1, 2, 27].

The property which is of interest here is that the following behaviour of σ_e is usually assumed:

$$\sigma_e(u) \begin{cases} = \text{const.} & \text{for } u \leq u_c, \\ > 0 & \text{for } u > u_c, \end{cases} \quad \sigma'_e(u) := \frac{d\sigma_e}{du} \begin{cases} = 0 & \text{for } u \leq u_c, \\ > 0 & \text{for } u > u_c, \end{cases} \quad (50)$$

where u_c is the so-called critical concentration or gel point, at which the solid flocs are assumed to touch each other. From (49), (50) and the assumptions on $f(u) = f_{bk}(u)$ we read off that $a(u) = 0$ for $u \leq u_c$ and $a(u) > 0$ for $u > u_c$ wherever $f(u) < 0$. Most notably, many, but not all, constitutive equations for σ_e imply a jump of σ_e' at $u = u_c$, which makes $a(u)$ discontinuous.

It should be mentioned that the postulate of a constitutive equation of the type $\sigma_e = \sigma_e(u)$ follows widespread usage in the engineering literature, see [2] and the references cited therein and recent handbooks on solid-liquid separation such as [29] and [30]. One should, however, bear in mind that this relationship is a strong (albeit in many cases useful) simplification, and that different approaches for σ_e , although altering the nature of the resulting model equation, could possibly describe better observed consolidation behaviour. In fact, several researchers recently proposed alternate equations for the effective solid stress function. Some of them suggest expressing σ_e as an integral (with respect to height) of a new concentration-dependent phenomenological function [31, 32] (see also [33]). It can be easily seen that in the present model framework this will lead again to a first-order equation, *i.e.* one essentially falls back to the equation

$$\frac{\partial u}{\partial t} + \frac{\partial f_{bk}(u)}{\partial x} = 0 \quad (51)$$

of Kynch's kinematic sedimentation theory [34], with all its well-known shortcomings. A different, and to our view potentially more promising approach was advanced by Zheng and Bagley [35, 36], who proposed an effective stress equation [35, Equation 18] that depends on both the value of the local solids concentration and its rate of change. Thereby the necessity to refer to a critical concentration is removed. However, the appropriate mathematical framework in which the resulting mathematical model should be studied still remains to be explored.

We briefly come back to condition (8) for Problem B (*i.e.*, we prescribe the total flux $\Psi(t)$ at $x = 1$) and show that (8) is satisfied for the most practically relevant choices of the functions $f_{bk}(\cdot)$ and $\sigma_e(\cdot)$. First, it is easy to see that in view of $q(\cdot) \leq 0$, it is sufficient to establish (8) for $q \equiv 0$. To be specific, and to focus on the main idea, we now assume that $f_{bk}(\cdot)$ is differentiable (as is the case in virtually all applications) and has a unique local minimum $0 < u_m < u_{\max}$, and that

$$\sigma_e'(u_c^+) := \lim_{u \downarrow u_c} \sigma_e'(u) > 0.$$

Typical examples for the model functions include the Michaels and Bolger [28] flux density function

$$f_{bk}(u) = v_\infty u (1 - (u/u_{\max}))^C, \quad v_\infty < 0, \quad C > 1, \quad (52)$$

and the 'power law' effective solid stress function (see *e.g.* [37])

$$\sigma_e(u) = \begin{cases} 0 & \text{for } u \leq u_c, \\ \sigma_0 ((u/u_c)^n - 1) & \text{for } u > u_c, \end{cases} \quad \sigma_0 > 0, \quad n > 1. \quad (53)$$

These model functions will be used in the first and the third numerical example presented below.

It is now easy to see that condition (9) and therefore condition (8) is satisfied in the case that $u_c \leq u_m$. Otherwise, we have to show that (8) also holds for $u_m < u \leq u_c$, *i.e.*, that

$$\xi a(u) \equiv -\xi \frac{f_{bk}(u)\sigma'_e(u)}{\Delta \varrho g u} \geq f'_{bk}(u) + M_g \quad \text{for } u_m < u \leq u_c \quad (54)$$

holds for suitable positive constants M_g and ξ . However, (54) can be easily established by setting

$$M_g = \max_{u \in [u_m, u_c]} f'_{bk}(u) > 0, \quad \xi = -\frac{2\Delta \varrho g u_c M_g}{f_{bk}(u_c)\sigma'_e(u_c^+)}.$$

Note that the assumption that $f_{bk}(\cdot)$ is differentiable is not essential here, *i.e.* we could also admit a function $f_{bk}(\cdot)$ that is only Lipschitz continuous.

4.2. NUMERICAL EXAMPLES

4.2.1. Comparison of first- and second-order schemes

For simplicity, we assume for this example that $q \equiv 0$ and that $n \in \mathbb{N}$. Noting that f_{bk} has a minimum at $u_m = u_{\max}/(C+1)$, we easily see that

$$f_{bk}^{\text{EO}}(u, v) = \begin{cases} f_{bk}(v) & \text{if } u \leq u_m, v \leq u_m, \\ f_{bk}(u) + f_{bk}(v) - f_{bk}(u_m) & \text{if } u > u_m, v \leq u_m, \\ f_{bk}(u_m) & \text{if } u \leq u_m, v > u_m, \\ f_{bk}(u) & \text{if } u > u_m, v > u_m \end{cases} \quad (55)$$

and that $A(u) = 0$ for $u \leq u_c$ and $A(u) = \mathcal{A}(u) - \mathcal{A}(u_c)$ for $u > u_c$, where

$$\mathcal{A}(u) = \frac{v_\infty \sigma_0}{\Delta \varrho g u_c^n} (1 - (u/u_{\max}))^C u^n \sum_{j=1}^n \left(\prod_{\ell=1}^j \frac{n+1-\ell}{C+\ell} \right) ((u_{\max}/u) - 1)^j. \quad (56)$$

Here we utilize the parameters $v_\infty = -2.7 \times 10^{-4} \text{ m s}^{-1}$, $C = 21.5$, $u_{\max} = 0.5$, $u_c = 0.07$, $\sigma_0 = 1.2 \text{ [Pa]}$ and $n = 5$ that have been determined for a flocculated Kaolin suspension whose settling behaviour was studied in [38]. Simulations of the same experiment with a slightly different set of parameters are presented in [39, 40]. Here, however, our interest is mainly focused on the errors introduced by the first- and second-order methods.

Figure 1 shows the difference between the numerical solutions calculated with $\theta = 0$ and $\theta = 1$ for the case $J = 200$. In addition, the errors versus J (referred to a reference solution calculated with $J = 2400$ and $\theta = 1$) at times $t = 2000 \text{ [s]}$, $t = 6000 \text{ [s]}$ and $t = 10000 \text{ [s]}$ have been plotted in Figure 2. As expected, we see that the second-order scheme performs better than the first-order scheme. Moreover, the accuracy of the second-order scheme seems to depend on the limiter function, *i.e.*, the value of θ , with $\theta = 1$ giving the best result in the present example. Observe that the largest difference between the first- and second-order schemes is seen for small times ($t = 2000$), *i.e.*, when the solution contains a strong discontinuity, and that it seems to decrease as t becomes large. We believe that this is related to accumulation error coming from the (only first-order) time integration.

In Figure 3, we show the numerical solution for $\Delta x = L/300$, $\theta = 0.5$ and $\text{CFL} = 0.98$ together with the measured iso-concentration lines (experimental data have been available for $t \leq 5000 \text{ [s]}$ only). We observe good approximation of the supernate/suspension interface, the rising sediment layer, and of the iso-concentration line for $u = 0.12$. Of course, due to the simple approach of the flux density function $f_{bk}(\cdot)$ adopted here, the agreement of simulated and measured data for the remaining iso-concentration lines is only qualitative.

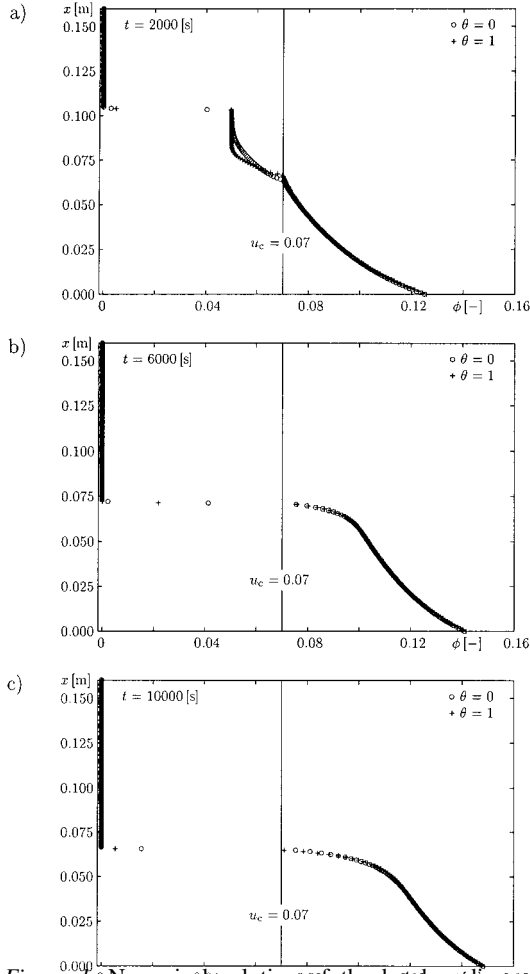


Figure 1. Numerical solution of the batch sedimentation problem: non-interpolated numerical values for $J = 200$ at a) $t = 2000$ [s], b) $t = 6000$ [s] and c) $t = 10000$ [s], calculated by the first-order ($\theta = 0$) and a second-order ($\theta = 1$) scheme.

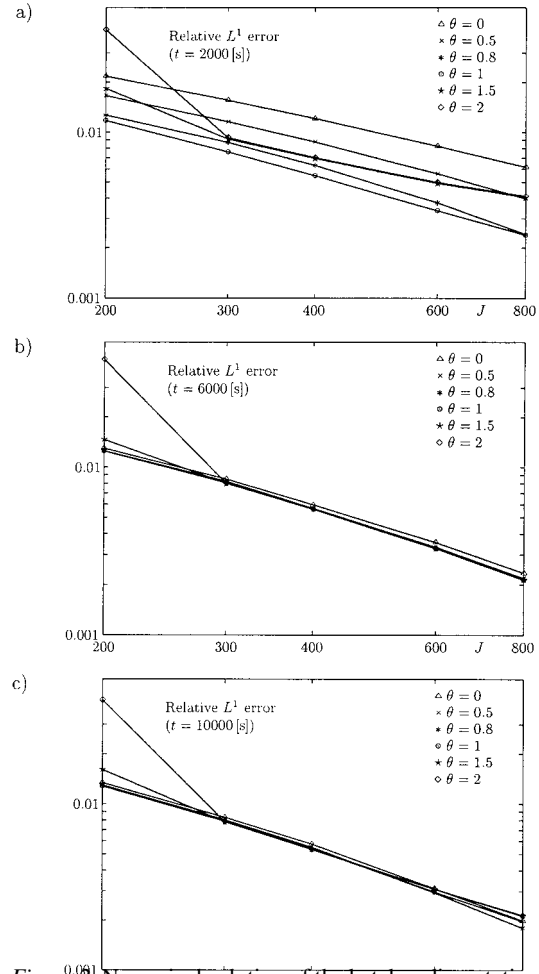


Figure 2. Numerical solution of the batch sedimentation problem: relative L^1 errors (as given in Table 1) at a) $t = 2000$ [s], b) $t = 6000$ [s] and c) $t = 10000$ [s] for different values of θ .

4.2.2. Comparison with experimental results

We now consider settling experiments performed by Holdich and Butt [41], see also the recent monograph by Rushton *et al.* [29]. In these experiments, suspensions of talc in tap water ($\Delta\rho = 1690$ [kg m⁻³]) at various initial concentrations were allowed to settle in a column. Concentration profiles were determined by conductivity measurements. From the published experimental data, Garrido *et al.* [42] determined the following constitutive equations:

$$f_{bk}(u) = \begin{cases} v_{\infty}(a_2 u^2 + a_1 u) & \text{for } u \leq u_M := (3b_1 - b_2)/(2b_2), \\ v_{\infty}(1 - u)^3/(b_1 - b_2 u) & \text{for } u_M < u < u_{\infty} := b_1/b_2, \end{cases}$$

$$\sigma_e(u) = \begin{cases} 0 & \text{for } u \leq u_c = 0.04, \\ \sigma_0 u^{\tilde{n}} & \text{for } u > u_c. \end{cases}$$

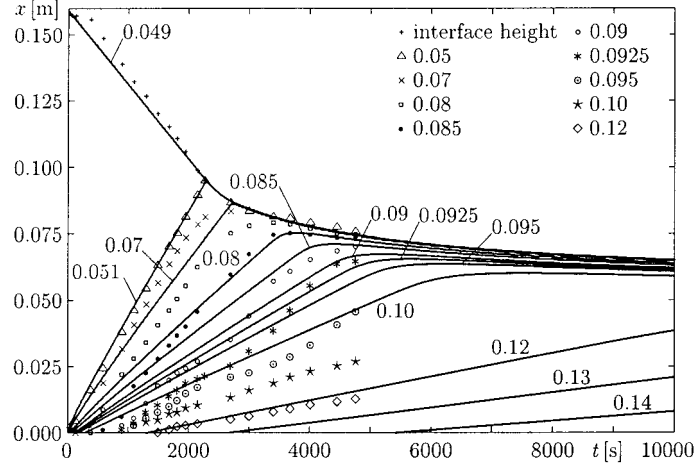


Figure 3. Simulation of a sedimentation experiment [38] with initial concentration $u_0 = 0.05$ and numerical parameters $\Delta x = L/300$, $\theta = 0.5$ and $\text{CFL} = 0.98$. The symbols correspond to the measured and the solid lines to the simulated iso-concentration lines.

where $v_\infty = -4.4 \times 10^{-6}$ [m/s] and $\sigma_0 = 2.1379 \times 10^7$ [Pa]. The value u_M is the local maximum of the expression $(1 - u)^3 / (b_1 - b_2 u)$. The linear denominator $b_1 - b_2 u$ comes from a corresponding approach for the Kozeny coefficient (see [41]). For the materials used in the experiment, the constants $b_1 = 12$, $b_2 = 32.5$ and hence $u_\infty \approx 0.3692$ and $u_M \approx 0.0538$ were found to be suitable [42]. The coefficients in the expression for $u \leq u_M$, $a_2 = -28.5004$ and $a_1 = 3.0693$, have been determined in such a way that f_{bk} is continuously differentiable. Since f_{bk} is also monotone, we obtain here $f_{bk}^{EO}(u_j^n, u_{j+1}^n) = f_{bk}(u_{j+1}^n)$. To make an explicit representation of the integrated diffusion coefficient $A(u)$ possible, we replace the exponent $\tilde{n} = 6.944$ determined in [42] by an integer n , e.g. $n = 7$, and obtain

$$A(u) = \begin{cases} 0 & \text{for } u \leq u_c, \\ \mathcal{A}_1(u) - \mathcal{A}_1(u_c) & \text{for } u_c < u \leq u_M, \\ \mathcal{A}_1(u_M) - \mathcal{A}_1(u_c) + \mathcal{A}_2(u) - \mathcal{A}_2(u_M) & \text{for } u_M < u < u_\infty, \end{cases}$$

where

$$\begin{aligned} \mathcal{A}_1(u) &= -\frac{v_\infty \sigma_0 n}{\Delta \rho g} \left(\frac{a_2}{n+1} u^{n+1} + \frac{a_1}{n} u^n \right), \\ \mathcal{A}_2(u) &= -\frac{v_\infty \sigma_0 n}{\Delta \rho g b_1} \left[\frac{(3u_\infty - 3u_\infty^2 + u_\infty^3)u^{n-1}}{n-1} + \frac{(u_\infty^2 - 3u_\infty)u^n}{n} + \frac{u_\infty u^{n+1}}{n+1} \right. \\ &\quad \left. + u_\infty^{n-1} (u_\infty - 1)^3 \left\{ \sum_{j=1}^{n-2} \binom{n-2}{j} \frac{((u/u_\infty) - 1)^j}{j} + \ln |(u/u_\infty) - 1| \right\} \right]. \end{aligned}$$

In Figures 4 and 5, we show numerical solutions calculated for the initial concentrations $u_0 = 0.052$, 0.072 and 0.112 with the parameters $J = 300$, $\theta = 0.5$ and $\text{CFL} = 0.98$. The values of u_0 correspond to the initial concentrations prepared in Holdich and Butt's settling experiments [41]. Figure 4 shows the simulated and some of the measured iso-concentration lines (t vs. x plots), while Figure 5 depicts the solutions as concentration profiles for selected

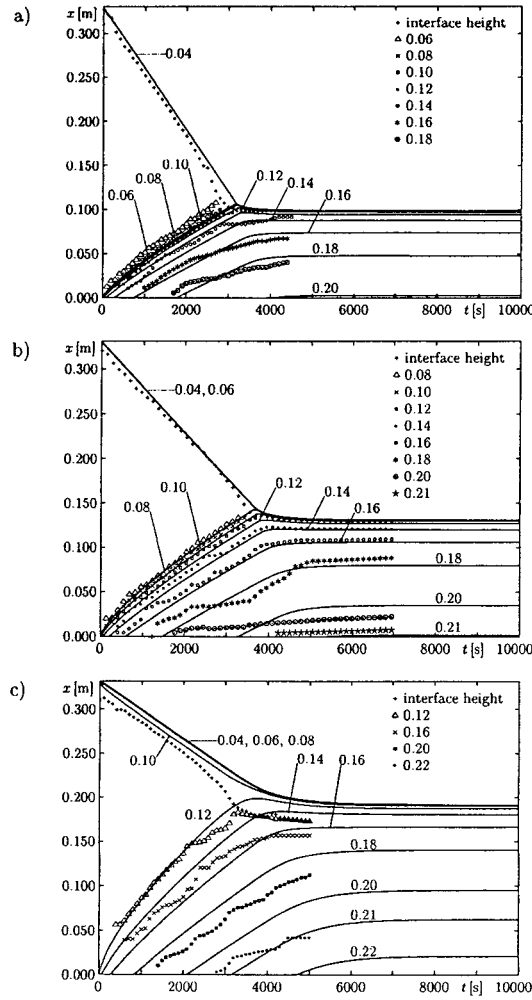


Figure 4. Simulation of a sedimentation experiment [41] with initial concentrations a) $u_0 = 0.052$, b) $u_0 = 0.072$ and c) $u_0 = 0.112$ and numerical parameters $\Delta x = L/300$, $\theta = 0.5$ and $CFL = 0.98$. The symbols correspond to the measured and the solid lines to the simulated iso-concentration lines.

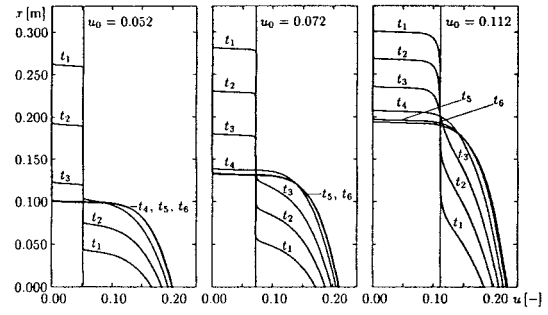


Figure 5. Concentration profiles of the numerical solutions shown in Figure 5 for $t_i = i \cdot 1000$ [s], $i = 1, \dots, 6$. The vertical line denotes the initial concentration.

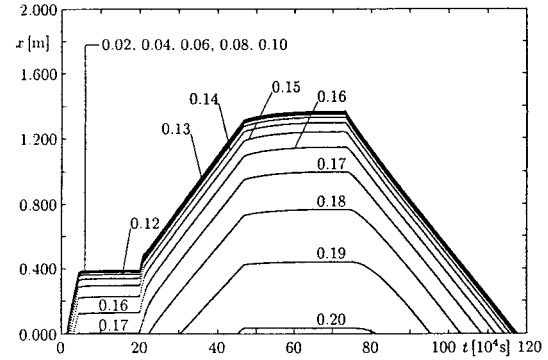


Figure 6. Numerical simulation of a continuous sedimentation-consolidation process.

times (u vs. x plots). Perhaps with the exception of the case $u_0 = 0.112$, we observe good agreement of experimental and measured data. This is, of course, mainly due to the care that has been applied in the determination of the function $f_{bk}(\cdot)$. In fact, Holdich and Butt [41] present numerical simulations for the cases $u_0 = 0.052$ and $u_0 = 0.112$ where the agreement is of similar quality. However, their solution technique is based on a different model formulation, and it is unclear whether their finite differencing admits type degeneracy.

Furthermore, we emphasize that the model function $f_{bk}(\cdot)$ used in this numerical example does *not* satisfy the assumptions of the mathematical analysis since it has a singularity at

$u = u_\infty$. Nevertheless, the presence of the diffusion term makes it possible to determine numerical solutions to Problem A with this flux density function.

4.2.3. Simulation of continuous sedimentation

We consider the model functions (52) and (53) with the parameters $v_\infty = -1.98 \times 10^{-4}$ [m/s], $C = 5.647$, $u_{\max} = 0.3$, $u_c = 0.1$, $\sigma_0 = 5.7$ [Pa] and $n = 9$, which approximate the model functions determined for a suspension of calcium carbonate, see [39, 43].

We assume that the sedimentation vessel, an Ideal Continuous Thickener (ICT) [44] of height $L = 2$ [m], is initially empty, *i.e.*, we set $u_0 \equiv 0$. At $x = 1$, we prescribe the feed flux $\Psi(t) = -8.55 \times 10^{-7}$ [m/s] for $0 \leq t \leq 200000$ [s]. We assume that the vessel is kept closed ($q = 0$), such that the ICT starts to fill up, until either $t = 45000$ [s] is reached or the concentration at $x = 0$ reaches the value $u(0, t) = 0.171$. At that moment, the vessel is opened, and we set $q(t) = -5.0 \times 10^{-6}$ [m/s] until $t = 200000$ [s]. Since now $\Psi(t) = 0.171 \times q(t)$, that is, the feed flux equals the discharge flux, the concentration profile assumes a steady state (see [45] for a detailed discussion of steady states).

At $t = 200000$ [s] we wish to change to a different steady state, characterized by the discharge concentration $u(0, t) = 0.201$, $q(t) = -1.5 \times 10^{-6}$ [m s⁻¹] and the corresponding feed flux $\Psi(t) = 0.201 \times q(t) = -3.015 \times 10^{-7}$ [m s⁻¹]. Since this steady state corresponds to a higher sediment level, we set $\Psi(t) = -3.015 \times 10^{-7}$ [m s⁻¹] for 200000 [s] $< t \leq 730000$ [s], but close the thickener (and thus produce an increase of the bottom concentration as well as a rise of the sediment level) until the desired discharge concentration $u(0, t) = 0.201$ is reached. At that moment (roughly, at $t = 470000$ [s]), $q(t)$ is changed from zero to the appropriate value $q(t) = -1.5 \times 10^{-6}$ [m s⁻¹], such that the concentration profile slowly attains the next desired steady state.

Finally, at $t = 730000$ [s], we decide to empty the ICT. Therefore the feed is stopped, *i.e.*, we set $\Psi(t) = 0$ for $t > 730000$ [s], but the value of $q(t)$ is not changed. We observe that the sediment level decreases at nearly constant speed, until all solids have left the ICT at $t \approx 1\,170\,000$ [s]. The simulation ends at $T = 1\,200\,000$ [s], which corresponds to roughly two weeks.

Figure 6 shows the iso-concentration lines corresponding to this simulation. Particular attention should be drawn to the fact that, in accordance with experience from engineering practice, the simulation illustrates that thickener operations with flocculated suspensions take place extremely slowly. This is due to the large time scale associated with the consolidation process. On the other hand, changes of the feed flux propagate very rapidly into the ICT as discontinuities or rarefaction waves in the hindered settling zone.

It should be commented that modelling continuous sedimentation as an initial-boundary-value problem (as proposed first by Petty [46] and Bustos *et al.* [47]) represents a strong simplification, since it is assumed that solids always travel downwards from $x = 1$. In practice, however, we will observe in many situations that solid flocs travel upwards from the feed level, entering the clarification zone. In that zone, the bulk flow of the mixture is directed upwards towards an overflow outlet. Consequently, an improved formulation of a continuous thickener should also include a clarification zone and be based on a discontinuous (with respect to x) flux function and a source term for the feed mechanism. The feed mechanism is then described by an additional source term. For the simpler case $\alpha_e \equiv 0$, corresponding to Kynch's theory [34], such thickener-clarifier models have been investigated by Diehl in a series of papers (see *e.g.* [48, 49, 50]).

5. Conclusions

In this paper, we have described a class of finite-difference schemes for initial-boundary-value problems of a strongly degenerate parabolic equation arising from the phenomenological theory of sedimentation-consolidation processes. We have shown that these schemes approximate the correct (entropy) solution of these problems, and that they can be employed to efficiently simulate batch and continuous sedimentation processes of flocculates suspensions.

The comparisons with experimental results are perhaps not so much a credit to the performance of the numerical schemes, rather than to the mathematical model: degenerate parabolic equations are the right extension of Kynch's well-known kinematical sedimentation theory [34], which leads to the first-order conservation law (51) and hence is unable to predict curved iso-concentration lines in the sediment layer.

Finally, this paper has highlighted the value of theoretical investigations related to existence and uniqueness questions for practitioners in the mentioned engineering applications. It has pointed out that no particular difficulties occur by combining two different mechanisms, that of sedimentation and that of compression, into one single field equation with a degenerating and even discontinuous coefficient. The formulation of the numerical scheme to solve this, which might be employed as a simulator for parameter identification, is rather straightforward. However, the mathematical analysis of the initial-boundary-value problem was necessary to prove that it indeed approximates the right weak, *i.e.* entropy solution. As is very clearly shown in [5, 16], this is *not* the case with similarly natural discretizations that work well for strictly parabolic equations with smooth coefficients, but that fail to converge to the right weak solution in the strongly degenerate discontinuous case.

One of the consequences of the mathematical and numerical analysis outlined here is that no special consideration of the evolving supernate-suspension and suspension-sediment interfaces or local data analysis is necessary for the simulation of the sedimentation-consolidation process. This sharply contrasts with different, more complicated treatments such as that in [51]: the authors of that paper essentially use the same model as that outlined in this paper, but use separate solution procedures for the hyperbolic and the parabolic compression part, which requires a manual graphical procedure, based on the frequent a priori assumption that characteristics emerge tangentially from the type-change interface, *i.e.* the sediment level.

Acknowledgements

We acknowledge financial support by the Sonderforschungsbereich 404 at the University of Stuttgart and by the Applied Mathematics in Industrial Flow Problems (AMIF) programme of the European Science Foundation (ESF).

References

1. R. Bürger, W.L. Wendland and F. Concha, Model equations for gravitational sedimentation-consolidation processes. *ZAMM* 80 (2000) 79–92.
2. M.C. Bustos, F. Concha, R. Bürger and E.M. Tory, *Sedimentation and Thickening*. Dordrecht: Kluwer Academic Publishers (1999) 304 pp.
3. R. Bürger and W.L. Wendland, Existence, uniqueness and stability of generalized solutions of an initial-boundary value problem for a degenerating quasilinear parabolic equation. *J. Math. Anal. Appl.* 218 (1998) 207–239.

4. R. Bürger, S. Evje and K.H. Karlsen, On strongly degenerate convection-diffusion problems modeling sedimentation-consolidation processes. *J. Math. Anal. Appl.* 247 (2000) 517–556.
5. S. Evje and K.H. Karlsen, Monotone difference approximations of BV solutions to degenerate convection-diffusion equations. *SIAM J. Numer. Anal.* 37 (2000) 1838–1860.
6. Z. Wu and J. Yin, Some properties of functions in BV_x and their applications to the uniqueness of solutions for degenerate quasilinear parabolic equations. *Northeastern Math. J.* 5 (1989) 395–422.
7. Z. Wu, A boundary value problem for quasilinear degenerate parabolic equations. Madison: MRC Technical Summary Report #2484, University of Wisconsin (1983) 13 pp.
8. R. Bürger and W.L. Wendland, Entropy boundary and jump conditions in the theory of sedimentation with compression. *Math. Meth. Appl. Sci.* 21 (1998) 865–882.
9. S.N. Kružkov, First order quasilinear equations in several independent variables. *Math. USSR Sb.* 10 (1970) 217–243.
10. A.I. Vol’pert, The spaces BV and quasilinear equations. *Math. USSR Sb.* 2 (1967) 225–267.
11. A.I. Vol’pert and S.I. Hudjaev, Cauchy’s problem for degenerate second order parabolic equations. *Math. USSR Sb.* 7 (1969) 365–387.
12. C. Bardos, A.Y. Le Roux and J.C. Nédélec, First order quasilinear equations with boundary conditions. *Comm. Part. Diff. Eqns.* 4 (1979) 1017–1034.
13. F. Dubois and P.G. Le Floch, Boundary conditions for nonlinear hyperbolic systems of conservation laws. *J. Diff. Eqns.* 71 (1988) 93–122.
14. J. Carrillo, Entropy solutions for nonlinear degenerate problems. *Arch. Rat. Mech. Anal.* 147 (1999) 269–361.
15. S. Evje and K.H. Karlsen, Viscous splitting approximation of mixed hyperbolic-parabolic convection-diffusion equations. *Numer. Math.* 83 (1999) 107–137.
16. R. Bürger, S. Evje, K.H. Karlsen and K.-A. Lie, Numerical methods for the simulation of the settling of flocculated suspensions. *Chem. Eng. J.* 80 (2000) 91–104.
17. H. Holden, K.H. Karlsen and K.-A. Lie, Operator splitting methods for degenerate convection–diffusion equations II: numerical examples with emphasis on reservoir simulation and sedimentation. *Comput. Geosci.*, to appear.
18. M.S. Espedal and K.H. Karlsen, Numerical solution of reservoir flow models based on large time step operator splitting algorithms. In: M.S. Espedal, A. Fasano and A. Mikelić (eds.) *Filtration in Porous Media and Industrial Application (Cetraro, Italy 1998)*. Berlin: Springer Verlag, Lecture Notes in Math. 1734 (2000) 9–77.
19. S. Evje and K.H. Karlsen, Discrete approximations of BV solutions to doubly nonlinear degenerate parabolic equations. *Numer. Math.* 86 (2000) 377–417.
20. S. Evje and K.H. Karlsen, Second order schemes for degenerate convection-diffusion equations. In preparation.
21. S. Evje and K.H. Karlsen, Degenerate convection-diffusion equations and implicit monotone difference schemes. In: M. Fey and R. Jeltsch (eds.) *Hyperbolic Problems: Theory, Numerics, Applications*. Basel: Birkhäuser Verlag. *Int. Ser. of Numer. Math.* 129 (1999) 285–294.
22. K.H. Karlsen and N.H. Risebro, Convergence of finite difference schemes for viscous and inviscid conservation laws with rough coefficients. *Math. Model. Numer. Anal.*, to appear.
23. K.H. Karlsen and N.H. Risebro, On the uniqueness and stability of entropy solutions of nonlinear degenerate parabolic equations with rough coefficients. Bergen: Applied Mathematics Report, University of Bergen, Norway (2000).
24. B. van Leer, Towards the ultimate conservative difference scheme. V. A second-order sequel to Godunov’s method. *J. Comput. Phys.* 32 (1979) 101–136.
25. B. van Leer, On the relation between the upwind-differencing schemes of Godunov, Engquist-Osher and Roe. *SIAM J. Sci. Statist. Comput.* 5 (1984) 1–20.
26. E.F. Toro, *Riemann Solvers and Numerical Methods for Fluid Dynamics*. Berlin: Springer-Verlag (1997) 592 pp.
27. R. Bürger and F. Concha, Mathematical model and numerical simulation of the settling of flocculated suspensions. *Int. J. Multiphase Flow* 24 (1998) 1005–1023.
28. A.S. Michaels and J.C. Bolger, Settling rates and sediment volumes of flocculated Kaolin suspensions. *Ind. Eng. Chem. Fund.* 1 (1962) 24–33.
29. A. Rushton, A.S. Ward and R.G. Holdich, *Solid-Liquid Filtration and Separation Technology*, Second Edition. Weinheim: Wiley-VCH (2000) 604 pp.

30. R.J. Wakeman and E.S. Tarleton, *Filtration: Equipment Selection, Modelling and Process Simulation*. Oxford: Elsevier Science (1999) 472 pp.
31. T. Dreher and B. Westrich, Experiments and simulations of sedimentation and consolidation of cohesive particles. Stuttgart: Preprint 99/09, Sonderforschungsbereich 404, University of Stuttgart (1999) 9 pp.
32. E.A. Toorman and H. Huysenstryt, Towards a new constitutive equation for effective stresses in consolidating mud. In: N. Burt, R. Parker and J. Watts (eds.) *Cohesive Sediments*. Chichester: Wiley (1997) pp. 121–132.
33. E.A. Toorman, Sedimentation and self-weight consolidation: constitutive equations and numerical modeling. *Géotechnique* 49 (1999) 709–726.
34. G.J. Kynch, A theory of sedimentation. *Trans. Farad. Soc.* 48 (1952) 166–176.
35. Y. Zheng and D.M. Bagley, Numerical simulation of batch settling process. *J. Environ. Eng.* 124 (1998) 953–958.
36. Y. Zheng and D.M. Bagley, Dynamic model for zone settling and compression in gravity thickeners. *J. Environ. Eng.* 125 (1999) 1007–1013.
37. K. Landman and L.R. White, Solid/liquid separation of flocculated suspensions. *Adv. Colloid Interf. Sci.* 51 (1994) 175–246.
38. F.M. Tiller, N.B. Hsyung, Y.L. Shen and W. Chen, CATSCAN analysis of sedimentation and constant pressure filtration. In: Proceedings of the Fifth World Congress on Filtration. Nice: Société Française de Filtration (1991), vol. 2, pp. 80–85.
39. R. Bürger, F. Concha and F.M. Tiller, Applications of the phenomenological theory to several published experimental cases of sedimentation processes. *Chem. Eng. J.* 80 (2000) 105–117.
40. R. Bürger, W.L. Wendland and F. Concha, Mathematical and numerical modelling of industrial gravity thickening. In: K.P. Holz, W. Bechteler, S.S.Y. Wang and M. Kawahara (eds.) *Advances in Hydro-Science and -Engineering vol.III: Proceedings of the 3rd International Conference on Hydro-Science and -Engineering, Cottbus/Berlin, Germany, August 31–September 3, 1998*. Carrier Hall: Center for Computational Hydro-science and Engineering, The University of Mississippi (1998) p. 222 (abstract, full length paper published on CD-ROM).
41. R.G. Holdich and G. Butt, Experimental and numerical analysis of a sedimentation forming compressible compacts. *Separ. Sci. Technol.* 32 (1997) 2149–2171.
42. P. Garrido, R. Bürger and F. Concha, Settling velocities of particulate systems: 11. Comparison of the phenomenological sedimentation-consolidation model with published experimental results. *Int. J. Mineral Process.* 60 (2000) 213–227.
43. J.J.R. Damasceno, H.M. Henrique and G. Massarani, Análise do comportamento dinâmico de um espessador Dorr-Oliver. In: *Proc. of the III Meeting of the Southern Hemisphere on Mineral Technology*, São Lourenço, MG, Brazil (1992) 675–689.
44. F. Concha and R. Bürger, Wave propagation phenomena in the theory of sedimentation. In: E.F. Toro and J.F. Clarke (eds.) *Numerical Methods for Wave Propagation*. Dordrecht: Kluwer Academic Publishers (1998) 173–196.
45. R. Bürger, M.C. Bustos and F. Concha, Settling velocities of particulate systems: 9. Phenomenological theory of sedimentation processes: numerical simulation of the transient behaviour of flocculated suspensions in an ideal batch or continuous thickener. *Int. J. Mineral Process.* 55 (1999) 267–282.
46. C.A. Petty, Continuous sedimentation of a suspension with a nonconvex flux law. *Chem. Eng. Sci.* 30 (1975) 1451–1458.
47. M.C. Bustos, F. Concha and W.L. Wendland, Global weak solutions to the problem of continuous sedimentation of an ideal suspension. *Math. Meth. Appl. Sci.* 13 (1990) 1–22.
48. S. Diehl, A conservation law with point source and discontinuous flux function modeling continuous sedimentation. *SIAM J. Appl. Math.* 56 (1996) 388–419.
49. S. Diehl, Dynamic and steady-state behaviour of continuous sedimentation. *SIAM J. Appl. Math.* 57 (1997) 991–1018.
50. S. Diehl, On boundary conditions and solutions for ideal thickener-clarifier units. *Chem. Eng. J.* 80 (2000) 119–133.
51. P. Diplas and A.N. Papanicolaou, Batch analysis of slurries in zone settling regime. *J. Environ. Eng.* 123 (1997) 659–667.